Published in final edited form as:
Angew Chem Int Ed Engl. 2013 April 15; 52(16): 4384–4388. doi:10.1002/anie.201207721.

On-Demand Drug Release System for *In Vivo* Cancer Treatment via Self Assembled Magnetic Nanoparticles**

Dr. Jae-Hyun Lee
Department of Chemistry Yonsei University Seoul 120-749 (Korea)

Dr. Kuan-Ju Chen
Department of Molecular and Medical Pharmacology Crump Institute for Molecular Imaging (CIMI) California NanoSystems Institute (CNSI) Institute for Molecular Medicine (IMED) University of California, Los Angeles Los Angeles, CA 90095-1770 (USA)

Seung-Hyun Noh
Department of Chemistry Yonsei University Seoul 120-749 (Korea)

Dr. Mitch André Garcia
Department of Molecular and Medical Pharmacology Crump Institute for Molecular Imaging (CIMI) California NanoSystems Institute (CNSI) Institute for Molecular Medicine (IMED) University of California, Los Angeles Los Angeles, CA 90095-1770 (USA)

Dr. Hao Wang [Prof.]
Department of Molecular and Medical Pharmacology Crump Institute for Molecular Imaging (CIMI) California NanoSystems Institute (CNSI) Institute for Molecular Medicine (IMED) University of California, Los Angeles Los Angeles, CA 90095-1770 (USA)

National Center for Nanoscience and Technology 11 Beiyitiao Zhongguancun Haidian District, Beijing, 100190 (P. R. China)

Dr. Wei-Yu Lin [Prof.]
Department of Molecular and Medical Pharmacology Crump Institute for Molecular Imaging (CIMI) California NanoSystems Institute (CNSI) Institute for Molecular Medicine (IMED) University of California, Los Angeles Los Angeles, CA 90095-1770 (USA)

Department of Medicinal and Applied Chemistry Kaohsiung Medical University 100, Shih-Chuan 1st Road, Kaohsiung, 80708 (Taiwan)

Heeyeong Jeong
Department of Chemistry Yonsei University Seoul 120-749 (Korea)

Brian Junoh Kong
Department of Molecular and Medical Pharmacology Crump Institute for Molecular Imaging (CIMI) California NanoSystems Institute (CNSI) Institute for Molecular Medicine (IMED) University of California, Los Angeles Los Angeles, CA 90095-1770 (USA)

David B. Stout [Prof.]
Department of Molecular and Medical Pharmacology Crump Institute for Molecular Imaging (CIMI) California NanoSystems Institute (CNSI) Institute for Molecular Medicine (IMED) University of California, Los Angeles Los Angeles, CA 90095-1770 (USA)

Jinwoo Cheon* **[Prof.]**

**This research was supported by NIH R21 GM098982 (HRT).

*jcheon@yonsei.ac.kr. *Phone: (+1) 310-794-1977; Fax: (+1) 310-206-8975 Web: http://tseng-lab.comhrtseng@mednet.ucla.edu.

Supporting information for this article is available on the WWW under http://www.angewandte.org.

Department of Chemistry Yonsei University Seoul 120-749 (Korea)

Hsian-Rong Tseng* **[Prof.]**
Department of Molecular and Medical Pharmacology Crump Institute for Molecular Imaging (CIMI) California NanoSystems Institute (CNSI) Institute for Molecular Medicine (IMED) University of California, Los Angeles Los Angeles, CA 90095-1770 (USA)

Keywords

supramolecular chemistry; magnetic nanoparticle; drug delivery; magnetic heat induction; molecular imaging

---

The intrinsic nature of small-molecule chemotherapeutics, including i) limited aqueous solubility, ii) systemic toxicity due to non-specific whole-body distribution, and iii) potential development of drug resistance after initial administration, compromises their treatment efficacy.[1] Recently, nanoparticle (NP)-based drug delivery systems have been considered as promising alternatives to overcome some of these limitations and begin to resolve obstacles in the disease management in clinical oncology.[2] The intraparticular space of a NP vector can be employed to package drug payloads without constrain associated with their solubility. Further, NP vectors exhibit enhanced permeability and retention (EPR) effects[3] that facilitate the differential uptake, leading to preferential spatio-distribution in tumor.[4] However, conventional NP drug delivery systems tend to passively release drug payloads, limiting the ability to release an effective drug concentration at a desired time window. Therefore, there is a need to develop next-generation NP drug delivery system such as a stimuli-responsive drug release system with a goal of achieving spatio-temporal control, by which an acute level of drug concentration can be delivered at the time point the NP vectors reach maximum tumor accumulation.[5] By doing so, it is expected to dramatically improve therapeutic effects in tumor and effectively reduce systematic toxicity at a minute drug dosage.[6]

Previously, we demonstrated a convenient, flexible, and modular self-assembled synthetic approach for the preparation of supramolecular nanoparticle (SNP) vectors from a collection of molecular building blocks via a multivalent molecular recognition between adamantane (Ad) and β-cyclodextrin (CD) motifs.[7] Such a self-assembled synthetic strategy enables control over the sizes, surface chemistry and payloads of SNP vectors for a wide range of diagnostic and therapeutic applications such as positron emission tomography (PET) imaging,[7] magnetic resonance imaging (MRI),[8] photothermal treatment,[9] as well as highly efficient delivery of genes,[10] transcription factors,[11] and drug-polymer conjugates.[12]

Herein, we introduce magnetothermally responsive doxorubicin-encapsulated supramolecular magnetic nanoparticles (Dox⊂SMNPs) as a unique on-demand drug delivery/release system (Scheme 1). The supramolecular synthetic strategy[7–12] was employed to prepare size-controllable Dox⊂SMNPs composed of the fluorescent anti-cancer drug, Dox, and four different molecular building blocks, including Ad-grafted polyamidoamine dendrimers (Ad-PAMAM), β-CD-grafted branched polyethylenimine (CD-PEI), Ad-functionalized polyethylene glycol (Ad-PEG) and 6-nm Ad-grafted $Zn_{0.4}Fe_{2.6}O_4$ superparamagnetic nanoparticle (Ad-MNP). The EPR effects are expected to drive preferential tumor accumulation of Dox⊂SMNPs,[4, 13] which constitutes the spatio-control of Dox⊂SMNPs. According to our design, the embedded magnetic NP (Ad-MNP) serves as a built-in transformer that converts radiofrequency external alternative magnetic field (AMF) into heat, allowing for stimuli-responsive drug release from Dox⊂SMNPs. In order to determine the ideal size of Dox⊂SMNPs for the proper spatial distribution and optimal

temporal point for the maximized tumor accumulation of Dox⊂SMNPs, ^{64}Cu-labeled Dox⊂SMNPs are prepared by incorporating radioisotope (i.e., $^{64}Cu^{2+}$) in the presence of DOTA ligand and then subjected to PET-based *in vivo* imaging studies. In parallel, an optimal AMF condition was determined by monitoring Dox release from Dox⊂SMNPs *in vitro*. Based on the results from both *in vivo* biodistribution and *in vitro* AMF optimization studies, we were able to design an optimized *in vivo* protocol for Dox⊂SMNPs to accomplish effective cancer therapy. Taken together, an acute level of drug concentration can be delivered to tumor with spatio-temporal control thus significantly reducing drug dosage.

The strong heat induction from zinc-doped MNP, due to its higher saturation magnetization value, makes this inorganic NP an ideal component for incorporation into our thermally responsive SNP vector.[14] We modified the 6-nm zinc-doped MNP with Ad, so that Ad-MNP (Figure 1a) can serve as one of molecular building blocks for incorporation into Dox⊂SMNPs via self-assembly. By fine-tuning the different ratios of the molecular building blocks, three sizes of Dox⊂SMNPs are prepared (70, 100, and 160 nm, Figure 1b–d). All three sizes of Dox⊂SMNPs have a narrow size distribution measured by light scattering, and Dox encapsulation efficiency is determined to be *ca*. 95% (see Figure S2).

A key physical parameter that determines the overall biodistribution pattern and therapeutic performance is the size of Dox⊂SMNPs.[2b, 15] We used micro-PET imaging to identify an optimal size of Dox⊂SMNPs with the highest retention in tumor.[6] 70-nm, 100-nm, and 160-nm ^{64}Cu-labeled (300 μCi) Dox⊂SMNPs were synthesized (see supporting information) and injected into DLD-1 tumor-bearing NU/NU mice via intravenous (*i.v.*) administration. The time dependent accumulation of the three Dox⊂SMNPs in the tumor versus whole body are summarized and plotted in Figure 1e. The results show that 70-nm Dox⊂SMNPs achieve their maximum tumor accumulation at 36 h post-injection, which is the critical time point for the optimal spatial distribution of Dox⊂SMNPs. The representative two-dimensional cross-sections of static filtered back-projection micro-PET images of the three Dox⊂SMNPs taken at 36 h post-injection are shown in Figure 1f–h, indicating that 70-nm Dox⊂SMNPs have the highest tumor-specific uptake among the three sizes; therefore, 70-nm Dox⊂SMNPs were chosen and utilized for further *in vitro* and *in vivo* studies. We note that the high signal measured in the liver should not be a major concern since it is presumably due to demetalation of ^{64}Cu from the DOTA ligand,[16] and thus does not accurately represent the location of Dox⊂SMNPs in that organ (see quantified biodistribution and clearance data in the supporting information).

The self-assembly of Ad-PAMAM, Ad-MNP, CD-PEI, and Ad-PEG generates SMNP vectors with intraparticular cationic hydrogel networks. Such hydrogel networks constitute a unique nano-environment that induces self-organization of Dox molecules driven by their intermolecular π–π stacking interactions.[17] As a result, the fluorescent signal of encapsulated Dox molecules is quenched almost completely (*ca*. 97%, see Figure S3) while associated with the SMNP vector. AMF is used as an external on-demand control to trigger the fast release of encapsulated Dox from the disassembled SMNP vector via magnetic heating.[9] Once released from the SMNP vector, the fluorescence of Dox molecules is restored. We use this photophysical property of Dox to investigate Dox⊂SMNPs' magnetically activated drug release performance as a function of AMF duration (500 kHz, 37.4 kA/m). Results show that the drug release from Dox⊂SMNPs nearly saturates with 10 min of AMF without raising the temperature of surrounding solution (see Figure S7b). When we apply multiple AMF pulses for a 2-min duration to the Dox⊂SMNPs with an 8-min interval (Figure 2a), approximately 50% of encapsulated Dox molecules are released in the first AMF pulse (Figure 2a, red line), while more Dox is released in a stepwise fashion after subsequent AMF pulses up to 7 or 8 pulses (50 min; Figure 2a, black line). Based on

these results, we selected a single pulse of AMF application with a 10-min duration as an effective AMF condition of DoxCSMNPs-based drug delivery system in further *in vitro* and *in vivo* studies, which can achieve on-demand release of an acute level of Dox concentration while avoiding unregulated drug release and thermal heating of surrounding medium.

In vitro on-demand release of Dox from 70-nm DoxCSMNPs were investigated for DLD-1 colorectal adenocarcinoma cell line with (Figure 2b, left column) and without (Figure 2b, right column) the application of a 10-min AMF (500 kHz, 37.4 kA/m). After the cells (1.5×10^4) are treated with 70-nm DoxCSMNPs (200 μg/mL treatment), minimal drug release with dim Dox fluorescence and no cell damage are observed (Figure 2b, right column). However, after exposure to AMF, blebbing and Dox fluorescence (red) is significantly increased (Figure 2b, left column). Also, nucleus fragmentations[18] and formation of apoptotic cell bodies are seen, demonstrating the consequence of effective Dox release from DoxCSMNPs under AMF application. A CCK-8 assay is used to quantify cell viability showing the decrease of viability to 30% after AMF application. Without the application of AMF, negligible cytotoxicity is observed and AMF alone has no effect on cell viability (Figure 2c).

Based on the systemic biodistribution results (optimal time point, i.e., 36 h post-injection, Figure 1e) and the *in vitro* drug release experiments (favorable AMF condition, i.e., 10 min, Figure 2), we designed an idealized *in vivo* treatment protocol of 70-nm DoxCSMNPs for cancer therapy. When the tumor volume of DLD-1 xenografted mice (n=3) reached 100 mm^3, DoxCSMNPs (70 nm, 150 μg/kg) were administered intravenously (day 0) followed by AMF treatment (10 min, 500 kHz, 37.3 kA/m) after 36 h post-injection. Anti-tumor efficacy results treated with DoxCSMNPs (w/ and w/o AMF) and other control studies (i.e., AMF only and PBS only) are summarized as plots of tumor volume over the course of treatment in Figure 3a. The control groups (i.e., DoxCSMNPs w/o AMF, AMF only, and PBS) do not show any statistically significant differences in tumor suppression (Figure 3a). The group treated with a single injection of DoxCSMNPs with applied AMF shows tumor suppression efficacy only up to day 7 (Figure 3a, red line). In contrast, the group treated with a double injection (day 0 and day 7) of DoxCSMNPs with AMF shows continued and effective inhibition of tumor growth (Figure 3a, black line). The tumor images of each group are shown in Figure 3b, which visually confirm the effective tumor suppression of the doubly injected DoxCSMNPs with AMF application. In addition, the drug-free vector (SMNPs w/o Dox) was administered following the same protocol, which gives similar results as control groups indicating that the effect of thermal heating by SMNP is negligible (see supporting information). It is notable that our DoxCSMNPs system only requires a low amount of drug (2.8 μg/kg Dox per injection) for tumor suppression, which is 3 orders of magnitude less than other NP systems (see supporting information, Table 1).[19]

In conclusion, we successfully demonstrate an on-demand drug delivery/release system that utilizes magnetothermally responsive DoxCSMNPs for highly effective *in vivo* cancer treatment. An optimized *in vivo* treatment protocol of DoxCSMNPs was designed after studying their biodistribution at a systemic level and evaluating *in vitro* trigger release of Dox with an optimal AMF condition. This on-demand drug release system utilized 1/1000 the drug dosage compared to existing protocols. We expect this cutting edge drug delivery/release system with spatio-temporal controllability may open up clinical opportunities for drug candidates that exhibit good therapeutic efficacy but fail toxicology testing by ensuring increased selectivity and reducing side effects.

Supplementary Material

Refer to Web version on PubMed Central for supplementary material.

References

[1]. Allen TM, Cullis PR. Science. 2004; 303:1818–1822. [PubMed: 15031496]

[2]. a) Davis ME, Chen Z, Shin DM. Nat. Rev. Drug. Discov. 2008; 7:771–782. [PubMed: 18758474] b) Petros RA, DeSimone JM. Nat. Rev. Drug. Discov. 2010; 9:615–627. [PubMed: 20616808] c) Wang AZ, Langer R, Farokhzad OC. Ann. Rev. Med. 2012; 63:185–198. [PubMed: 21888516] d) Tassa C, Shaw SY, Weissleder R. Acc. Chem. Res. 2011; 44:842–852. [PubMed: 21661727]

[3]. Torchilin V. Adv. Drug. Deliver. Rev. 2011; 63:131–135.

[4]. a) Matsumura Y, Maeda H. Cancer Res. 1986; 46:6387–6392. [PubMed: 2946403] b) Dufort S, Sancey L, Coll JL. Adv. Drug. Deliver. Rev. 2012; 64:179–189.

[5]. a) Ge J, Neofytou E, Cahill TJ, Beygui RE, Zare RN. ACS Nano. 2012; 6:227–233. [PubMed: 22111891] b) Yan H, Teh C, Sreejith S, Zhu L, Kwok A, Fang W, Ma X, Nguyen KT, Korzh V, Zhao Y. Angew. Chem. 2012; 124:8498–8502.Angew. Chem. Int. Ed. 2012; 51:8373–8377.

[6]. a) Harris TJ, von Maltzahn G, Derfus AM, Ruoslahti E, Bhatia SN. Angew. Chem. 2006; 118:3233–3237.Angew. Chem. Int. Ed. 2006; 45:3161–3165.b) Wu G, Mikhailovsky A, Khant HA, Fu C, Chiu W, Zasadzinski JA. J. Am. Chem. Soc. 2008; 130:8175–8177. [PubMed: 18543914] c) Desert A, Chaduc I, Fouilloux S, Taveau JC, Lambert O, Lansalot M, Bourgeat-Lami E, Thill A, Spalla O, Ravaine S, Duguet E. Poly. Chem. 2012; 3:1130–1132.d) Agarwal A, Mackey MA, El-Sayed MA, Bellamkonda RV. ACS Nano. 2011; 5:4919–4926. [PubMed: 21591812] e) Pradhan P, Giri J, Rieken F, Koch C, Mykhaylyk O, Doblinger M, Banerjee R, Bahadur D, Plank C. J Control Release. 2010; 142:108–121. [PubMed: 19819275]

[7]. Wang H, Wang ST, Su H, Chen KJ, Armijo AL, Lin WY, Wang YJ, Sun J, Kamei K, Czernin J, Radu CG, Tseng HR. Angew Chem. 2009; 121:4408–4412.Angew. Chem. Int. Ed. 2009; 48:4344–4348.

[8]. Chen KJ, Wolahan SM, Wang H, Hsu CH, Chang HW, Durazo A, Hwang LP, Garcia MA, Jiang ZK, Wu L, Lin YY, Tseng HR. Biomaterials. 2011; 32:2160–2165. [PubMed: 21167594]

[9]. Wang ST, Chen KJ, Wu TH, Wang H, Lin WY, Ohashi M, Chiou PY, Tseng HR. Angew. Chem. 2010; 122:3865–3869.Angew. Chem. Int. Ed. 2010; 49:3777–3781.

[10]. a) Wang H, Chen KJ, Wang ST, Ohashi M, Kamei KI, Sun J, Ha JH, Liu K, Tseng HR. Chem. Commun. 2010; 46:1851–1853.b) Wang H, Liu K, Chen KJ, Lu YJ, Wang ST, Lin WY, Guo F, Kamei KI, Chen YC, Ohashi M, Wang MW, Garcia MA, Zhao XZ, Shen CKF, Tseng HR. ACS Nano. 2010; 4:6235–6243. [PubMed: 20925389] c) Liu K, Wang H, Chen KJ, Guo F, Lin WY, Chen YC, Phung DL, Tseng HR, Shen CKF. Nanotechnology. 2010; 21

[11]. Liu Y, Wang H, Kamei K, Yan M, Chen KJ, Yuan QH, Shi LQ, Lu YF, Tseng HR. Angew. Chem. 2011; 123:3114–3118.Angew. Chem. Int. Ed. 2011; 50:3058–3062.

[12]. Chen KJ, Tang L, Garcia MA, Wang H, Lu H, Lin WY, Hou S, Yin Q, Shen CKF, Cheng JJ, Tseng HR. Biomaterials. 2012; 33:1162–1169. [PubMed: 22074663]

[13]. Acharya S, Sahoo SK. Adv. Drug. Deliver. Rev. 2011; 63:170–183.

[14]. a) Yoo D, Lee JH, Shin TH, Cheon J. Acc. Chem. Res. 2011; 44:863–874. [PubMed: 21823593] b) Lee JH, Jang JT, Choi JS, Moon SH, Noh SH, Kim JW, Kim JG, Kim IS, Park KI, Cheon J. Nat. Nanotechnol. 2011; 6:418–422. [PubMed: 21706024] c) Noh SH, Na W, Jang JT, Lee JH, Lee EJ, Moon SH, Lim Y, Shin JS, Cheon J. Nano Lett. 2012; 12:3716–3721. [PubMed: 22720795] d) Thomas CR, Ferris DP, Lee JH, Choi E, Cho MH, Kim ES, Stoddart JF, Shin JS, Cheon J, Zink JI. J. Am. Chem. Soc. 2010; 132:10623–10625. [PubMed: 20681678] f) Jang JT, Nah H, Lee JH, Moon SH, Kim MG, Cheon J. Angew. Chem. 2009; 121:1260–1264.Angew. Chem. Int. Ed. 2009; 48:1234–1238.

[15]. Cabral H, Matsumoto Y, Mizuno K, Chen Q, Murakami M, Kimura M, Terada Y, Kano MR, Miyazono K, Uesaka M, Nishiyama N, Kataoka K. Nat. Nanotechnol. 2011; 6:815–823. [PubMed: 22020122]

[16]. a) Suckow C, Kuntner C, Chow P, Silverman R, Chatziioannou A, Stout D. Mol. Imaging Biol. 2009; 11:100–106. [PubMed: 18679755] b) Stout D, Chatziioannou A, Lawson T, Silverman R, Gambhir S, Phelps M. Mol. Imaging Biol. 2005; 7:393–402. [PubMed: 16261425]

[17]. Boswell CA, Sun XK, Niu WJ, Weisman GR, Wong EH, Rheingold AL, Anderson CJ. J. Med. Chem. 2004; 47:1465–1474. [PubMed: 14998334]

[18]. a) Erukova VY, Krylova OO, Antonenko YN, Melik-Nubarov NS. BBA-Biomembranes. 2000; 1468:73–86. [PubMed: 11018653] b) Hayakawa E, Furuya K, Ueno H, Kuroda T, Moriyama M, Kondo A. Chem. Pharm. Bull. 1991; 39:1009–1012.c) Yu MK, Jeong YY, Park J, Park S, Kim JW, Min JJ, Kim K, Jon S. Angew. Chem. 2008; 120:5442–5445.Angew. Chem. Int. Ed. 2008; 47:5362–5365.

[19]. Zoli W, Ulivi P, Tesei A, Fabbri F, Rosetti M, Maltoni R, Giunchi DC, Ricotti L, Brigliadori G, Vannini I, Amadori D. Breast Cancer Res. 2005; 7:R681–R689. [PubMed: 16168113]

[20]. a) Zhang W, Guo ZY, Huang DQ, Liu ZM, Guo X, Zhong HQ. Biomaterials. 2011; 32:8555–8561. [PubMed: 21839507] b) Agarwal A, Mackey MA, El-Sayed MA, Bellamkonda RV. ACS Nano. 2011; 5:4919–4926. [PubMed: 21591812] c) Liu Z, Fan AC, Rakhra K, Sherlock S, Goodwin A, Chen XY, Yang QW, Felsher DW, Dai HJ. Angew. Chem. 2009; 121:7804–7808.Angew. Chem. Int. Ed. 2009; 48:7668–7672.

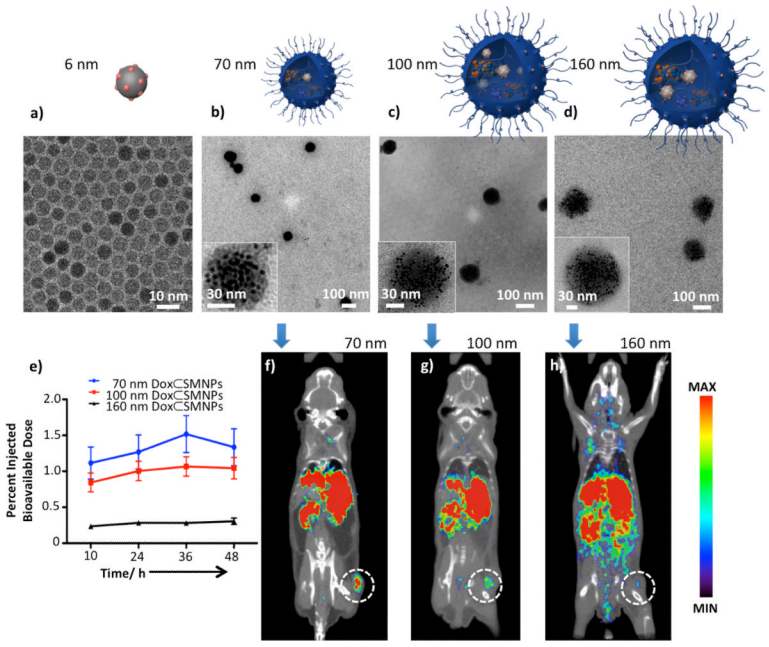

Figure 1.

Characterization and biodistribution of DoxCSMNPs. a–d) Transmission electron microscope (TEM) images of a) 6-nm Ad-MNP and DoxCSMNPs with various sizes of b) 70 ± 9, c) 96 ± 7, and d) 161 ± 8 nm. Insets: Higher magnification TEM images of each DoxCSMNPs. e) Time dependent accumulation of the three DoxCSMNPs in the tumor versus whole body of NU/NU mice measured by micro-PET (n=3). f–h) 2-D micro-PET cross-sections images, created using filtered back-projection, of mice bearing DLD-1 tumor (n=3) at 36 h post-injection of 70-nm, 100-nm, and 160-nm ^{64}Cu-labeled DoxCSMNPs; each image was scaled to its own maximum. The 70-nm DoxCSMNPs show the highest tumor-specific uptake among the three studies.

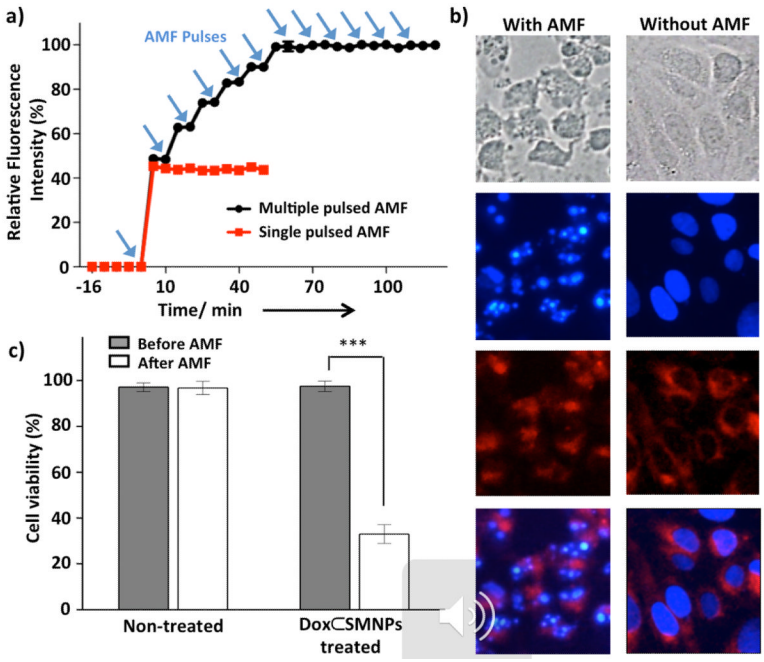

Figure 2.

In vitro drug release and therapeutic efficacy of 70-nm DoxCSMNPs. a) Dox release profiles upon the application of AMF in either multiple pulses (black line; 2 min of pulse duration with 8 min of non-pulsed intermittence) or as a single pulse (red line; 2 min of pulse duration). Approximately 50% of encapsulated Dox molecules release in the first AMF pulse and the rest of Dox releases stepwise in subsequent AMF pulses (** $p \leq 0.01$). b) Fluorescence microscope images of DLD-1 colon cancer cells treated with DoxCSMNPs with (left) and without (right) the application of a 10-min continuous AMF (500 kHz, 37.4 kA/m). Images from top to bottom: Differential interference contrast (DIC) image showing the cell morphology; DAPI stained image showing the nuclei; Dox fluorescence indicating the presence of Dox; merged image of DAPI and Dox. Dox molecules are released from DoxCSMNPs upon AMF application and then entered into nuclei, which leads to cell apoptosis. Scale bar: 10 μm. c) Cell viability results of DLD-1 cells treated with and without DoxCSMNPs before and after application of AMF for 10 min via CCK–8 assay (*** $p \leq 0.001$).

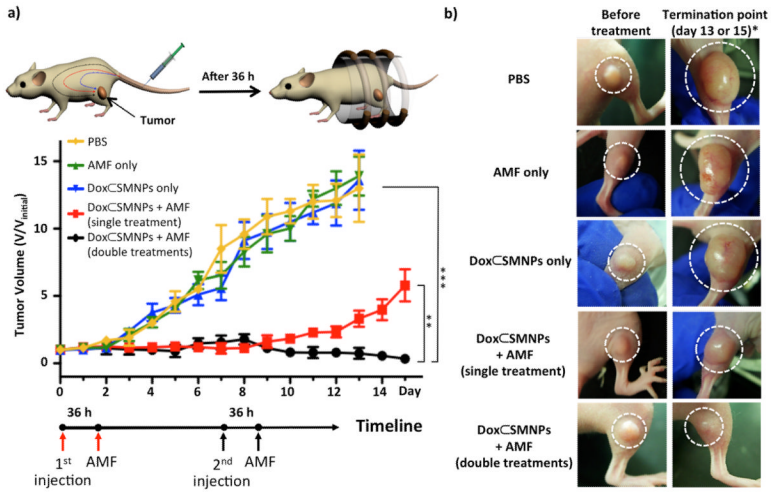

Figure 3.

Evaluation of *in vivo* therapeutic efficacy. a) Treatment scheme of DoxCSMNPs in mouse and results of tumor volume change over the course of treatment (15 days) in DLD-1 xenografted mice (n=3) treated with DoxCSMNPs (w/ and w/o application of AMF), and other controls (AMF only and PBS only). All injections were done on day 0 (and day 7 for the double injection group) when the tumor volume reached 100 mm^3; AMF application was performed at 36 h post-injection. The best tumor suppression result was observed in the group treated with a double injection of DoxCSMNPs with AMF application. The group treated with single injection of DoxCSMNPs with AMF, and the other control groups (i.e., treated with DoxCSMNPs only, AMF only and PBS) show either lesser degree or none of tumor suppression effects (** $p \leq 0.01$; *** $p \leq 0.001$). b) Tumor images of groups treated with DoxCSMNPs w/ and w/o application of AMF and other controls, before treatment (left panels) and at the termination point (right panels). The termination point of the experiment occurred either on day 15 or when the tumor volume reached 1500 mm^3.

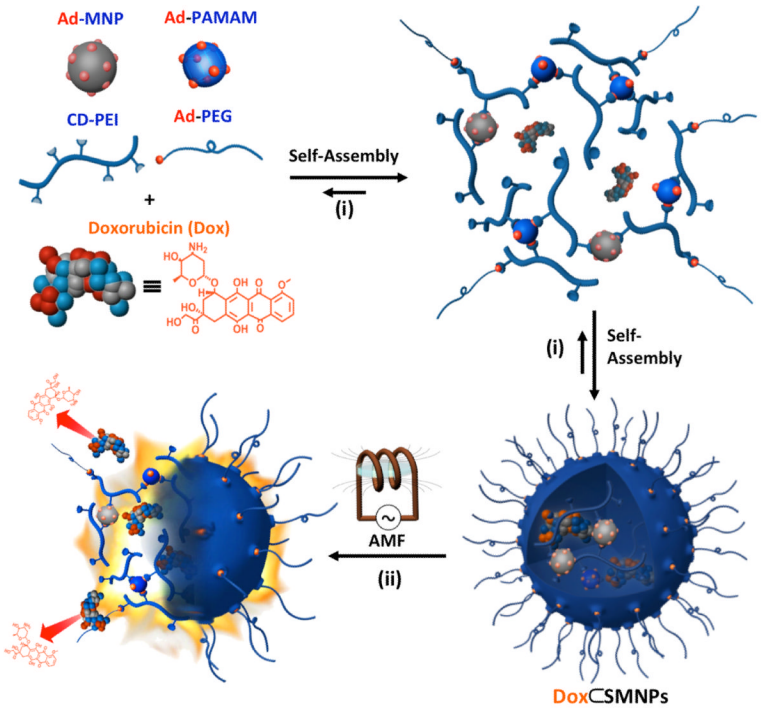

Scheme 1.

Schematic illustration summarizing the molecular design, self-assembly and function of magnetothermally responsive doxorubicin (Dox)-encapsulated supramolecular magnetic nanoparticles (DoxCSMNPs). i) The self-assembled synthetic strategy is employed for the preparation of DoxCSMNPs, which is made from a fluorescent anti-cancer drug (Dox) and four molecular building blocks: Ad-PAMAM, 6-nm Ad-grafted $Zn_{0.4}Fe_{2.6}O_4$ superparamagnetic nanoparticle (Ad-MNP), CD-PEI, and Ad-PEG. ii) The embedded Ad-MNP serves as a built-in heat transformer that triggers the burst release of Dox molecules from the magnetothermally responsive SMNP vector, achieving on-demand drug release upon the remote application of an alternative magnetic field (AMF).